Appl Microbiol Biotechnol
DOI 10.1007/s00253-016-7995-5



# *Penicillium roqueforti* PR toxin gene cluster characterization

**Pedro I. Hidalgo**[1] · **Elisabeth Poirier**[1] · **Ricardo V. Ullán**[2] · **Justine Piqueras**[1] · **Laurence Meslet-Cladière**[1] · **Emmanuel Coton**[1] · **Monika Coton**[1]

Received: 31 August 2016 / Revised: 2 November 2016 / Accepted: 5 November 2016


**Abstract** PR toxin is a well-known isoprenoid mycotoxin almost solely produced by *Penicillium roqueforti* after growth on food or animal feed. This mycotoxin has been described as the most toxic produced by this species. In this study, an in silico analysis allowed identifying for the first time a 22.4-kb biosynthetic gene cluster involved in PR toxin biosynthesis in *P. roqueforti*. The pathway contains 11 open reading frames encoding for ten putative proteins including the major fungal terpene cyclase, aristolochene synthase, involved in the first farnesyl-diphosphate cyclization step as well as an oxidoreductase, an oxidase, two P450 monooxygenases, a transferase, and two dehydrogenase enzymes. Gene silencing was used to study three genes (ORF5, ORF6, and ORF8 encoding for an acetyltransferase and two P450 monooxygenases, respectively) and resulted in 20 to 40% PR toxin production reductions in all transformants proving the involvement of these genes and the corresponding enzyme activities in PR toxin biosynthesis. According to the considered silenced gene target, eremofortin A and B productions were also affected suggesting their involvement as biosynthetic intermediates in this pathway. A PR toxin biosynthesis pathway is proposed based on the most recent and available data.

**Keywords** Mycotoxins · PR toxin · *Penicillium roqueforti* · Gene silencing · Biosynthesis pathway

## Introduction

Filamentous fungi are important microorganisms in both the agriculture and food sectors. In this context, they can be divided into two main categories: filamentous fungi with a negative impact, associated with feed or food spoilage (e.g., silage, cereals, bakery products, cheese,…) (Fink-Gremmels 2008; Hymery et al. 2014; Rasmussen et al. 2010; Storm et al. 2014), and those with a positive impact used for raw material (of vegetal or animal origin) transformation (e.g., tempeh, Starzynska-Janiszewska et al. 2012; miso, Okado et al. 2015; shoyu, Abe et al. 2006; dry sausages, Castellari et al. 2010; or mold-ripened cheeses, Gripon 1999).

*Penicillium roqueforti* is of particular interest in this context, as this species can belong to either category according to the considered food or feed matrix. Indeed, this species plays an important technological role during the well-known blue-veined cheese production via intense enzymatic activities involved in texture modification, aroma and flavor production as well as contributing to the typical cheese vein color due to conidial pigmentation. However, this species can also be a contaminant in other cheese types such as grated cheeses or hard pressed cheeses (Cantor et al. 2004; Dumay and Jalain 1982; Gripon 1999; Scott 1986). It is a widely spread bakery product contaminant (Lavermicocca et al. 2003; Lund et al. 1996) and is also the main fungal spoiler of silage used for animal feed (Boysen et al. 2000; Storm et al. 2010). Furthermore, this species is also known for its potential to produce secondary metabolites including mycotoxins (Hymery et al. 1996; Martin and Coton 2017) that may have a toxicological effect on animals or consumers (Hymery et al. 2014). In

**Electronic supplementary material** The online version of this article (doi:10.1007/s00253-016-7995-5) contains supplementary material, which is available to authorized users.

✉ Monika Coton
monika.coton@univ-brest.fr

[1] Université de Brest, EA 3882 Laboratoire Universitaire de Biodiversité et d'Ecologie Microbienne, IBSAM, ESIAB, Technopôle Brest-Iroise, Plouzané, 29280 Brest, France

[2] mAbxience, Upstream Production, Parque Tecnológico de León, Julia Morros s/n, Armunia, 24009 León, Spain

Published online: 05 December 2016

particular, *P. roqueforti* can produce three well-known mycotoxins, namely PR toxin, mycophenolic acid (MPA), and roquefortine C (ROQ C) (Nielsen et al. 2006; O'Brien et al. 2006; Rasmussen et al. 2010; Gillot et al. 2016; Martin and Coton 2017). Noteworthy, *P. roqueforti* mycotoxin-related outbreaks have not been reported except for PR toxin contamination in animal feed (Le Bars and Le Bars 1989; Scudamore and Livesey 1998; Still et al. 1972; Veselý et al. 1981), and to the best of our knowledge, these mycotoxin levels in food or feed are not regulated.

Among the three main *P. roqueforti* mycotoxins, PR toxin is of particular interest, as it is only produced by a reduced number of Penicillia, mainly *P. roqueforti*, but it was also listed to be produced by *Penicillium chrysogenum* by Frisvad and Samson (2004), while other mycotoxins can often be produced by several members of the same genus or sometimes by different genera. This mycotoxin was isolated and partially characterized by Chang et al. in 1993, and 2 years later, its chemical structure was fully elucidated (Wei et al. 1975). It corresponds to a bicyclic sesquiterpene derived from farnesyl pyrophosphate (FPP) and aristolochene belonging to the eremophilane class. PR toxin is considered to be the most toxic metabolite produced by *P. roqueforti* in regard to human health (Polonelli et al. 1978; Storm et al. 2014; Wei et al. 1979), and its toxicity was also confirmed by experimental studies showing its lethal effect in rats, mice, and cats (Chen et al. 1982).

This mycotoxin has been described to be unstable during cheese manufacture due to microaerophilic conditions and amino compounds present (Chang et al. 1993; Scott and Kanhere 1979) and to be degraded into the less toxic PR-imine, PR acid, and/or PR-amide compounds (Chang et al. 1993, 1996). However, *P. roqueforti* contamination in silage, maize, or other food and feed products can pose a safety risk and potentially have both health and economic impacts.

From a genetic point of view, while biosynthetic pathways for RoqC (Kosalková et al. 2015) and MPA (Del-Cid et al. 2016; Gillot et al. 2016) have been fully elucidated in *P. roqueforti*, this is not the case for PR toxin. Hidalgo et al. (2014) partially characterized the PR toxin cluster by RNA interference gene silencing. In the latter study, silencing of four genes including the *ari1* gene coding for an aristolochene synthase (sesquiterpene cyclase) and three genes encoding for a putative quinone oxidase and two dehydrogenases, respectively, produced a drastic reduction in PR toxin production. The aristolochene synthase is a monomeric sesquiterpene cyclase. Noteworthy, the crystal structure determined by Caruthers et al. (2000) was the first fungal terpenoid cyclase structure described. In addition to the already known aristolochene synthase (encoded by *ari1*) identified as responsible for FPP to aristolochene cyclization, Hidalgo et al. (2014) proposed that the quinone oxidase would be one of the enzymes responsible for the transformation of non-oxygenated aristolochene to the trioxygenated EreB. The two dehydrogenases were shown to be responsible for the last two steps of the biosynthetic route involved in PR toxin: the conversion of EreA to EreC (oxidation of the side chain of C-12 to form an alcohol group) and the oxidation of this alcohol group to an aldehyde group to form PR toxin. Considering the obtained results by Hidalgo et al. (2014) and previous results (Chang et al. 1991; Moreau et al. 1980; Brock and Dickschat 2013), a biosynthetic pathway for PR toxin production was proposed. More recently, Riclea and Dickschat (2015) showed, via multiple $^{13}$C-labeling feeding experiments, that 7-*epi*-neopetasone is a newly identified pathway intermediate and also proposed a hypothetical biosynthesis pathway.

In this study, the recently sequenced and annotated *P. roqueforti* FM164 genome sequence was used to search for supplementary genes putatively involved in the PR toxin biosynthetic cluster. Characterization of the *P. roqueforti* PR toxin biosynthetic cluster was extended by studying three other genes using RNA interference to determine their potential involvement in PR toxin production.

## Materials and methods

### Strains and culture conditions

The *P. roqueforti* ATCC 48936 (CECT 20485) strain used in this study was originally isolated in the USA, in 1930, from *Roquefort* cheese (Modler et al. 1974; Shetty and Gaertner 1975) and has the ability to produce PR toxin (Chang et al. 1991). It was routinely grown in solid Power sporulation medium (Casqueiro et al. 1999) for 5 days at 28 °C.

The parental strain and transformants were grown in yeast extract sucrose -corn extract medium (YESC) buffered at pH 4.0 with phosphate-citrate buffer, as this medium was shown to stimulate PR toxin production (Chang et al. 1998). YESC contained 1% yeast extract, 7.5% sucrose, and 20% (*v*/*v*) of corn extract. Corn extract was prepared by boiling 1 kg of fresh corn grains in 1.5 l of distilled water for 60 min. The extract was filtered through a cotton layer. The filtrate (corn extract) was then adjusted to a total volume of 1 l with distilled water. Fifty milliliters of YESC medium were then placed in a 250-ml flask, inoculated with 1 ml of a *P. roqueforti* spore suspension ($10^8$ spores ml$^{-1}$), and incubated under static conditions for 7 days at 24 °C.

### In silico study

Genes putatively involved in the PR toxin biosynthetic cluster were identified on the recently annotated genome *P. roqueforti* FM164 provided by Pr. Joëlle Dupont from the French National Museum of Natural History (MNHN). To do so, an in silico study was performed by searching for ORFs in the

upstream and downstream flanking regions of the *ari*1 sequence published by Proctor and Hohn (1993). The ORF Finder tool from NCBI (Altschul et al. 1990) was also used to analyze putative intron and exon regions in each identified ORF. Different blasts (tblastn, blastn, blastp, blastx) were also performed to search for homologies in GenBank and determine putative protein functions.

### PR toxin biosynthetic cluster gene mapping in two *P. roqueforti* strains

Gene mapping in *P. roqueforti* FM164 and *P. roqueforti* ATCC 48936 was performed to confirm if no differences in gene organization and synteny occurred between strains. Six primer pairs were designed to amplify intergenic regions between ORFs (orf4–orf5, orf5–orf6, orf6–orf8, orf8–orf9, orf9–orf10, orf10–orf11) and are listed in Supplementary Table S1. PCR amplifications were carried out in molecular biology-grade water, 1× buffer, 0.2 mM dNTPs, 2 mM $MgCl_2$, 0.2 mM of each primer, 0.5 U of GoTaq DNA polymerase (Promega, Madison, USA), and 50–100 ng genomic DNA as template. PCR amplifications were performed using a peqSTAR 2X Gradient Thermocycler (PEQLAB Biotechnologie GMBH, Erlangen, Germany) with the following program: 95 °C for 5 min, then 35 cycles of 95 °C for 30 s, 55 °C for 30 s, and 72 °C for 2 min followed by a final extension at 72 °C for 10 min. The obtained PCR products were then run on a 0.8% (*w*/*v*) agarose gel in 1X Tris Borate EDTA (TBE) and sequenced (Eurofins, Germany).

### Plasmid constructions for ORF5, ORF6, and ORF8 gene silencing

Cloning constructions were all performed by integration of an amplified partial sequence of a target gene of *P. roqueforti* ATCC 48936 in the *Nco*I site of pJL43RNAi vector (Ullán et al. 2008). The primer pairs F-SORF5/R-SORF5, F-SORF6/R-SORF6, and F-SORF8/R-SORF8 (Supplementary Table S1) were used to amplify exonic fragments of 350 bp (nucleotides 201 to 350), 380 bp (nucleotides 214 to 593), and 402 bp (nucleotides 200 to 601) from the ORF5, ORF6, and ORF8, respectively. The PCR reactions contained molecular biology-grade water, 1× buffer, 0.2 mM dNTPs, 2 mM $MgCl_2$ (ORF5 and ORF8) and 2.5 mM $MgCl_2$ (ORF6), 0.2 mM of each primer, 0.5 U of GoTaq DNA polymerase (Promega, Madison, USA), and 50–100 ng genomic DNA as template. PCR amplifications were performed using a peqSTAR 2× Gradient Thermocycler (PEQLAB Biotechnologie GMBH, Erlangen, Germany) with the following program: 95 °C for 5 min, then 35 cycles of 95 °C for 30 s, 57 °C (ORF5) and 66 °C (ORF6 and ORF8) for 30 s, and 72 °C for 30 s followed by a final extension at 72 °C for 10 min. The obtained PCR products were then digested with the *Nco*I enzyme and cloned into pJL43RNAi to obtain the pSORF5-RNAi, pSORF6-RNAi, and pSORF8-RNAi plasmids, respectively.

### *P. roqueforti* protoplast preparation

*P. roqueforti* protoplasts were obtained using the protocol described by Hidalgo et al. (2014) with some minor modifications. Conidia were collected by scraping the *P. roqueforti* culture grown in the solid Power sporulation medium into physiologic solution (NaCl 0.9% *w*/*v*). Approximately 1 ml of conidia suspension was added to 100 ml of YES medium in a 500-ml flask to reach a final concentration of $10^7$ conidia/ml culture medium. The flask was incubated at 28 °C with agitation at 200 rpm for 20 to 24 h until the size of the mycelia was about ten times the diameter of the spore. The mycelium was then collected by filtration using a sterile nylon filter and washed two times with 0.9% NaCl to eliminate the remaining culture medium and ungerminated spores. The mycelium was suspended in 50 ml of 50 mM TPP buffer (potassium phosphate buffer with 0.7 M KCl at pH 5.8). One milliliter of $MgSO_4$ 1 M and 0.5 ml of DL-dithiothreitol (DTT) 1 M (Sigma) were then added. The DTT treatment was performed at 25 mM at 28 °C for 1 h with constant stirring at 150 rpm in order to reduce the disulfide bridges in and between proteins helping the hyphal separation and subsequent enzymatic treatment. The mycelium was then collected by filtration and washed with TPP buffer to eliminate the remaining DTT. Ten milliliters of a sterile lytic enzyme solution (Sigma-Aldrich) diluted in TPP at a concentration of 40 mg $ml^{-1}$ was prepared in a 10-ml tube. The washed mycelium was suspended in 10 ml TPP buffer to homogeneity and transferred to a 250-ml flask and then 10 ml of lytic enzymes were added (final concentration 20 mg $ml^{-1}$). The mixture was incubated at 28 °C for 2 to 4 h in an orbital shaker at 40 rpm. Protoplast release was monitored by observation of samples by optical microscopy every 30 min after 1.5-h incubation. After protoplast release, the suspension was filtered through a cloth filter (Miracloth, Millipore) with a 22–25-μm pore size; the recovered eluent was then centrifuged at 2500 rpm for 5 min at 4 °C. The pellet was washed two times with KCM buffer (0.7 M KCl, 50 mM $CaCl_2$, 10 mM 2-(*N*-morpholino)ethanesulfonic acid at pH 5.8). Protoplasts were finally suspended in KCM buffer with 10% (*v*/*v*) PCM (50% polyethylene glycol 6000, 50 mM CaCl2, 10 mM 2-(*N*-morpholino)ethanesulfonic acid at pH 5.8) solution to a final concentration of $2.5 \times 10^8$ protoplasts/ml (counted in a Malassez chamber).

### *P. roqueforti* transformation

The transformation of *P. roqueforti* protoplasts was performed as previously described by Ullán et al. (2007) using up to 10-μl plasmid DNA solution (1 μg $\mu l^{-1}$). Transformants were

selected in solid Czapek minimal medium supplemented with sorbitol (1 M) and phleomycin (5 μg $ml^{-1}$) as osmotic stabilizer and selection agent, respectively. Control conditions were included in these experiments by not adding DNA to determine protoplast regeneration, by checking the appearance of reverting colonies, and by adding the plasmid alone to ensure that no modifications to growth or metabolism occurred due to plasmid integration.

### Metabolite extraction from *P. roqueforti* cultures

The secondary metabolites produced in liquid medium by the different *P. roqueforti* strains (ATCC 48936 used as a control and the obtained transformants) were extracted by liquid-liquid extraction as follows. Twenty milliliters of the fermentation broth were separated from the mycelium by filtration and placed in a 50-ml tube. Then, 20 ml of ethyl acetate were added and the suspension was mixed vigorously for 1 min. The two phases were separated by centrifugation at 6000 rpm for 5 min at 4 °C, and the organic phase was collected in a new tube. A second extraction was performed with 20 ml of ethyl acetate, and the two organic extracts were pooled together and then dried using a rotary evaporator (IKA-Werke RV-10). The dried samples were redissolved in 5 ml of $H_2O$ + 0.1% formic acid/acetonitrile (50/50%) and analyzed by liquid chromatography-mass spectrometry/quadrupole time-of-flight (LC-MS/Q-TOF).

### PR toxin identification and chromatographic analysis

The extracted metabolites were separated and identified by LC-MS/Q-TOF analysis. An Agilent 1290 Series HPLC system with binary pump and degasser, well plate autosampler with thermostat, and a thermostated column compartment were used for the separation. Dry extracts were resuspended in 1 ml of $H_2O$ + 0.1% formic acid/acetonitrile (50:50%) and filtered using 0.2-μm filters before injection. Two microliters of each sample was injected in the system, and the separation was performed using a ZORBAX Extend C18 column (2.1 × 50 mm and 1.8 μm, maximum pressure 600 bar) (Agilent, France). The column was maintained at 35 °C throughout the entire chromatographic run. The flow rate was set to 0.3 ml $min^{-1}$ using as mobile phase: solvent A (Milli-Q water + 0.1% formic acid + 10 mM ammonium formate) and solvent B (100% acetonitrile). Solvent B was maintained at 10% for the first 4 min, followed by a gradient of 10–100% of B during 18 min. Finally, solvent B was maintained at 100% for 5 min. Compound detection was performed using an Agilent 6530 Series Accurate-Mass Quadrupole Time-of-Flight (Q-TOF) mass spectrometer with an electrospray ionization (ESI) source operated in positive and negative ion modes. Mass spectrometer conditions were as follows: capillary voltage, 4 kV; source temperature, 325 °C; nebulizer pressure, 50 psig; drying gas, 12 l $min^{-1}$, and ion range, 100 to 1000 *m*/*z*. PR toxin standard (provided by Dr. Olivier Puel, INRA Toulouse) was used as reference compound to ensure accurate quantification (*m*/*z* 321.13 in ESI+ mode, not detected in ESI− mode) and stored at −20 °C in acetonitrile. LC-MS/Q-TOF calibrations were performed before each run following the mass spectrometer manufacturer's instructions.

### RNA extraction and gene expression studies

RNA extractions were performed on 4-day fresh mycelium cultures from the *P. roqueforti* parental strain and one representative transformant for each gene target using the NucleoSpin RNA Plant Kit (Macherey Nagel, France) according to the manufacturer's instructions. Extracted RNA samples then underwent a second DNase treatment using the RapidOut DNA Removal Kit (Thermo Fisher Scientific, Inc., Waltham, MA, USA) according to the manufacturer's instructions to ensure that no genomic DNA was left. RNA samples were migrated on 0.8% *w*/*v* agarose gels to ensure their integrity and also quantified using a Nanodrop ND 1000 spectrophotometer (Thermo Fisher Scientific, Inc., Waltham, MA, USA). All samples were conserved at −80 °C. RT-qPCR experiments were performed using the iTaq Universal SYBR Green One-Step Kit (Bio-Rad, Hercules, CA, USA) in 10-μl final volumes as recommended by the manufacturer. PCR mixtures were carried out in molecular biology-grade water in the presence of 1× iTaq Universal SYBR Green reaction mix, 200 nM of each primer, 1× iScript reverse transcriptase, and 15 ng of RNA template. Amplifications were performed using a Bio-Rad CFX96 Real-Time PCR Thermocycler (Bio-Rad, Hercules, CA, USA) with the following thermal cycling protocol: 50 °C for 10 min, 95 °C for 1 min, [95 °C for 10 s; 60 °C for 30 s] × 40 cycles, following by a melt curve analysis 65–95 °C (0.5 °C increment with 5 s/step). Phosphofructokinase (*pfkA*) was selected as the most adequate reference gene based on recent study on *P. roqueforti* involving RT-qPCR experiments (Gillot et al. 2016), and the primers used were pfkA-F/pfkA-R (Supplementary Table S1). RT-qPCR primer couples for each gene target were also designed to study changes in *P. roqueforti* gene expression (Supplementary Table S1). All experiments were performed using three biological replicates and in triplicate. Control experiments excluding iScript reverse transcriptase were also performed on each RNA sample to ensure that no contaminating DNA could be detected. Gene expression data were then analyzed using the Livak method (Livak and Schmittgen 2001) and confidence intervals (95%) were determined for all experiments. Different mean value groups were compared to control values according to the least significant difference (LSD) test of multifactor ANOVA analysis using Statgraphics Plus for Windows (version 1.4 StatPoint Technologies, Inc., Warrenton).

## Results

### Identification of the PR toxin biosynthetic cluster in *P. roqueforti* FM164

The aristolochene synthase (ARI1) protein sequence (Proctor and Hohn 1993a) was used to perform an in silico search for the putative biosynthetic gene cluster involved in PR toxin production using the *P. roqueforti* FM164 annotated genome (GenBank assembly accession no. GCA_000513255.1). After identification of the corresponding *ari1* gene, the upstream and downstream flanking regions were analyzed using ORF Finder (NCBI). An approximately 25-kb region containing 11 ORFs, one of which (ORF2) coincided with the *ari*1 gene (Fig. 1), was identified in this species for the first time. The characteristics and putative function of the proteins encoded by these 11 ORFs are presented in Table 1. All coding sequences could be assigned to a putative protein function (between 91 to 100% protein sequence identities with known protein sequences in GenBank), except for ORF7, and included the known sesquiterpene cyclase and aristolochene synthase (ORF2), as well as dehydrogenase, oxidoreductase, oxidase, transferase, and multiple P450 monooxygenase-type enzymes. Noteworthy, comparison to genome databanks showed similarities in terms of gene synteny and protein homologies with two other technologically important *Penicillium* species, namely *Penicillium rubens* (penicillin producer) Wisconsin 54-1255 and *Penicillium camemberti* (soft ripened cheese production) FM013 (Table 1). Interestingly, *P. rubens* has been described as a PR toxin-producing species contrary to *P. camemberti*. One notable difference among the three species was observed for *P. roqueforti* ORF7 gene orientation (opposite 5′ to 3′ orientation in *P. rubens* and *P. camemberti*) coding for a 186 aa protein of unknown function in *P. rubens* and described to potentially correspond to an outer membrane protein in *P. roqueforti*. However, further studies will be required to elucidate whether this putative protein is indeed functional. Another notable difference was also observed for *P. roqueforti* ORF11 that contained a stop codon upstream of the one found in the other two species, thereby truncating this protein in the 3′ region in *P. roqueforti* (Fig. 1). Finally, according to Cheeseman et al. (2014) genome annotations, ORF9 in *P. camemberti* would encode an N-terminal truncated version of a P450 cytochrome monooxygenase (357 aa versus 509 aa in the two other species) that may explain the non-PR toxin production by *P. camemberti*. However, this and the involvement of ORF9 in this biosynthetic pathway should be further studied.

### Silencing of ORF5, ORF6, and ORF8

As the involvement of ORF2 (*ari1*) and three other ORFs (ORF1, ORF3, and ORF4) (Fig. 1) in PR toxin biosynthesis was recently confirmed (Hidalgo et al. 2014). In this study, three other genes (ORF5, ORF6, and ORF8) putatively coding for two P450 monooxygenases (ORF5, ORF6) and an acetyltransferase (ORF8) identified in this biosynthetic gene cluster were selected for gene silencing based on their putative functional assignation (Table 1) and their position in the cluster. As the high PR toxin producer *P. roqueforti* ATCC 48936 strain was selected for gene silencing, the first step consisted in confirming that no organizational differences existed with the biosynthetic gene cluster identified in the *P. roqueforti* FM164 genome. To do so, gene mapping was first performed using primers which amplify the intergenic regions between the different ORFs (orf4–orf5, orf5–orf6, orf6–orf8, orf8–orf9, orf9–orf10, orf10–orf11) (Supplementary Table S1, Supplementary Fig. S1). The sizes of the amplification products of intergenic segments spanning from gene to gene coincided between both strains (Supplementary Fig. S1). These results confirmed the identical cluster organization between

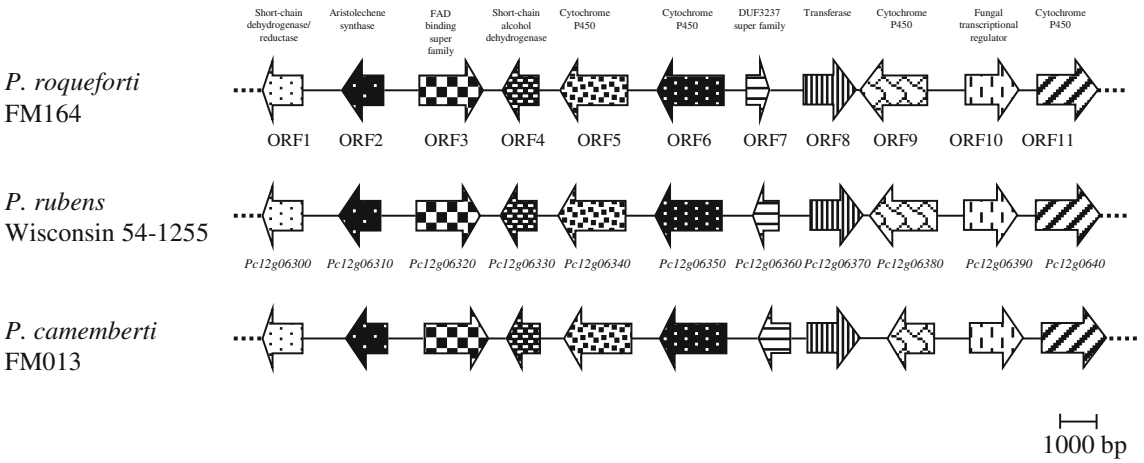


**Fig. 1** Physical map of 11 genes identified in the *P. roqueforti* FM164 genome putatively involved in PR toxin biosynthesis compared to those identified in *P. rubens* Wisconsin 54-1255 and *P. camemberti* FM013 annotated genome sequences

**Table 1** Characteristics of the proteins encoded by the PR toxin production pathway gene cluster *P. roqueforti* FM164

| | Location in nucleotide sequence | G+C (%) | Predicted protein (aa/kDa[a]/pI[a]) | Conserved domain[b] | Proposed function | % Identity[c] | Accession no.. | Organism |
|---|---|---|---|---|---|---|---|---|
| ORF1 | CDM31314 (Proq02g040180) | 54.38 | 340/36,558.43/5.45 | Retinol-DH_like_ SDR_c-like | Short-chain dehydrogenase/ reductase SDR | 96 | XP_002557572 | *P. rubens* |
| ORF2 | CDM31315 (Proq02g040190) | 52.17 | 342/39,191.57/5.21 | Terpene cyclase non-plant C1 | Aristolochene synthase | 100 | Q03471 | *P. roqueforti* |
| ORF3 | CDM31316 (Proq02g040200) | 51.63 | 512/54,663.32/4.85 | FAD binding 4 superfamily | Quinone oxidase domain | 96 | XP_002557474 | *P. rubens* |
| ORF4 | CDM31317 (Proq02g040210) | 53.63 | 329/35,588.84/6.33 | ADH_SDR_c-like | Short-chain alcohol dehydrogenase | 98 | XP_002557475 | *P. rubens* |
| ORF5 | CDM31318 (Proq02g040220) | 49.75 | 540/61,388.70/7.32 | p450 superfamily | Oxidation of non-activated hydrocarbons | 96 | XP_002557476 | *P. rubens* |
| ORF6 | CDM31319 (Proq02g040230) | 51.67 | 579/65,685.86/8.95 | p450 superfamily | Oxidation of non-activated hydrocarbons | 97<br>97 | XP_002557477<br>CRL18801 | *P. rubens*<br>*P. camemberti* |
| ORF7 | CDM31320 (Proq02g040240) | | 186/20,807.81/5.17 | DUF3237 superfamily | Outer membrane protein, beta-barrel | 100 | CDM31320 | *P. roqueforti* |
| ORF8 | CDM31322 (Proq02g040260) | 50.42 | 471/53,129.56/5.98 | Condensation superfamily | Transferase | 96 | CRL18798 | *P. camemberti* |
| ORF9 | CDM31323 (Proq02g040270) | 48.38 | 509/57,736.64/8.41 | p450 superfamily | Oxidation of non-activated hydrocarbons | 97 | XP_002557480 | *P. rubens* |
| ORF10 | CDM31324 (Proq02g040280) | 50.59 | 458/49,794.63/5.34 | GAL4 | Fungal transcriptional regulatory protein, N-terminal | 91 | CRL18795 | *P. camemberti* |
| ORF11 | CDM31325 (Proq02g040290) | 48.94 | 480/53,912.52/5.86 | p450 superfamily | Oxidation of non-activated hydrocarbons | 98 | XP_0022557482 | *P. rubens* |

[a] Theoretical molecular weight and isoelectrical point as estimated by the "Compute pI/Mw tool" (http://www.expasy.ch/tools/pi_tool.html)

[b] Identified by the "NCBI Conserved Domain Search" tool (http://www.ncbi.nlm.nih.gov/Structure/cdd/wrpsb.cgi)

[c] Identical amino acid (aa) percentage between the predicted sequence and the closest sequence in GenBank using BlastP

the two *P. roqueforti* strains; therefore, the PR toxin-producing ATCC 48936 strain was used for all experiments.

Concerning the gene silencing strategy, the pSORF5-RNAi, pSORF6-RNAi, and pSORF8-RNAi silencing vectors were constructed by inserting an exonic fragment of each target gene between the convergent promoters (*gpd*A and *pcb*C) of the pJL43RNAi plasmid (Ullán et al. 2008). The three silencing plasmids and the vector pJL43RNAi (as negative control) were used to transform freshly prepared protoplasts of *P. roqueforti* ATCC 48936. Positive transformants were selected by resistance to phleomycin (5 μg $ml^{-1}$), as this concentration fully inhibits growth of the untransformed *P. roqueforti* protoplasts as determined in preliminary tests. Several transformants for each of the silencing vectors were analyzed to confirm the correct integration, without rearrangement, of the silencing cassette in the *P. roqueforti* genome. Confirmation of transformants was performed by two approaches: specific PCR and Southern blotting. Total DNAs from spores of the phleomycin-resistant transformants were first analyzed by PCR using the FPpcbC and RPgpdA primers (Supplementary Table S1), which amplify the exonic fragment inserted between the two convergent PpcbC and PgpdA promoters. These two promoters are absent in *P. roqueforti*. Silencing vectors and the *P. roqueforti* ATCC 48936 parental strain were used as positive and negative controls, respectively. All amplifications were in accordance with the expected results for pSORF5-RNAi, pSORF6-RNAi, and pSORF8-RNAi as well as control conditions (data not shown). Selected positive transformants were then confirmed by Southern hybridization using an internal region of each of the exonic fragments as probes (Fig. 2). A 772-bp fragment of PpcbC was also used as a probe for the strains transformed with pJL43RNAi alone. Total DNA of each transformant was digested with *Sal*I (for ORF5, ORF6 and pJL43RNAi) or with *Pvu*I and *Eco*RI (for ORF8). These enzymes allowed releasing the endogenous gene and silencing cassette integrated in the

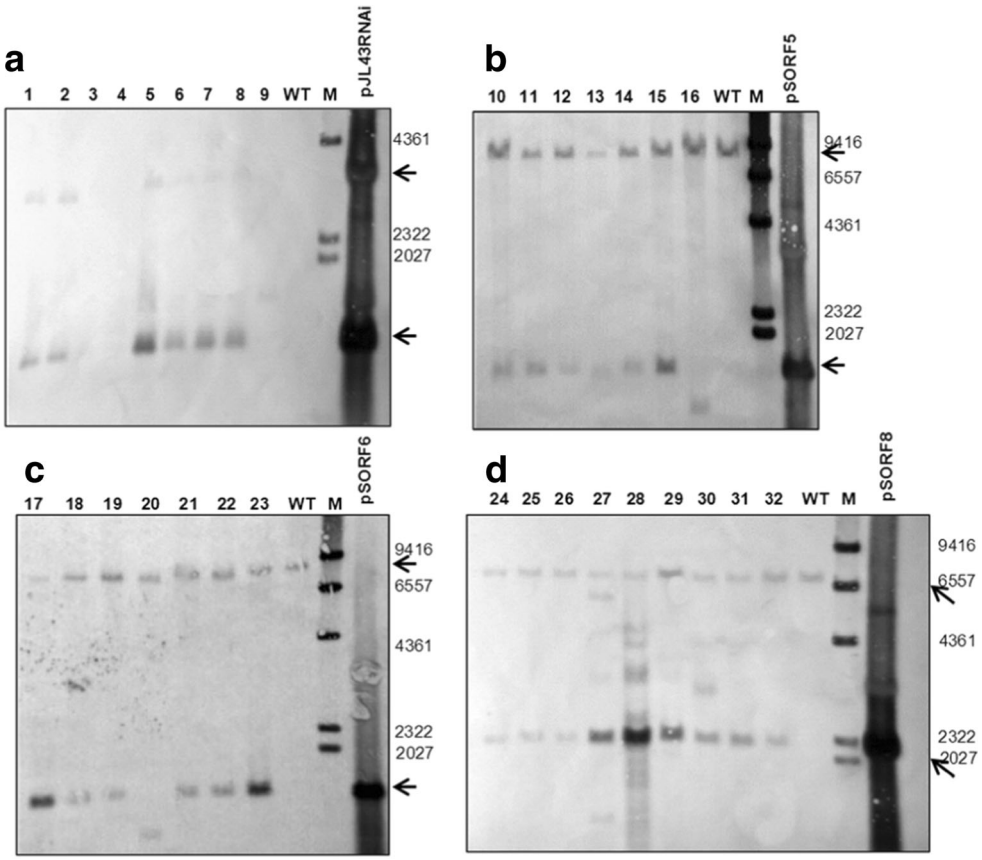


**Fig. 2** Southern hybridization of control pJL43RNAi (**a**), silenced ORF5 (**b**), ORF6 (**c**), and ORF8 (**d**). *Line 1*: tSpJL-04, *2*: tSpJL-05, *3*: tSpJL-07, *4*: tSpJL-08, *5*: tSpJL-09, *6*: tSpJL-10, *7*: tSpJL-11, *8*: tSpJL-13, *9*: tSpJL-14, *10*: tSorf5-01, *11*: tSorf5-03, *12*: tSorf5-06, *13*: tSorf5-10, *14*: tSorf5-13, *15*: tSorf5-14, *16*: tSorf5-15, *17*: tSorf6-04, *18*: tSorf6-05, *19*: tSorf6-07, *20*: tSorf6-08, *21*: tSorf6-09, *22*: tSorf6-10, *23*: tSorf6-11, *24*: tSorf8-03, *25*: tSorf8-04, *26*: tSorf8-11, *27*: tSorf8-12, *28*: tSorf8-13, *29*: tSorf8-14, *30*: tSorf8-15, 31: tSorf8-18, *32*: tSorf8-19. *WT*: *P. roqueforti* ATCC 48936, *M*: lambda DNA/*Hin*dIII marker. *Arrows* indicate the endogenous gene (*upper arrow*) and/or the integrated silencing cassette containing the target gene fragment (*lower arrow*). Numbers are in base pairs

genome for each plasmid construction without internal cuts. As for PCR confirmation test, silencing vectors and the *P. roqueforti* ATCC 48936 parental strain were included in each experiment as positive and negative controls, respectively. A size correspondence was observed between the bands observed in each positive transformant and those corresponding to silencing plasmids. No exogenous band was observed in the untransformed control strain (Fig. 2). As expected, these hybridizations also revealed the presence of the endogenous ORF5, ORF6, and ORF8 copies (bands of 8154, 8154, and 6766 bp, respectively) in each strain including the untransformed control. The pJL43RNAi transformants (Fig. 2) presented a band corresponding to the integration of the PpcbC and PgpdA fragments (1116 bp). No band was observed in the parental strain, as the pcbC promoter is absent in *P. roqueforti*.

## Growth study

As mycotoxin production can be linked to fungal biomass production and therefore to avoid any bias, we studied if the positive transformant growth was affected by integration of the silencing cassettes. To do so, a growth study was performed using two solid media, Czapek yeast autolysate (CYA) and YES agar, for the different transformants in comparison to the untransformed parental strain, *P. roqueforti* ATCC 48936. Radial growth (by measuring growth in at least two directions) was followed every 24 h until the mycelium reached the border of the plate. All growth experiments were performed in triplicate.

No changes in growth were observed between the transformants and control strains except for one transformant, torf5-10, for both media (Supplementary Figs. S2 and S3). Although transformants tSorf5-01, tSorf5-13, and tSorf8-04 showed slightly lower but non-significant radial growth on CYA medium, no differences in radial growth were observed in YES medium (Supplementary Figs. S2 and S3). As no significant differences were observed for the tested media, these transformants were included in the metabolic studies. Transformants tSorf5-01, tSorf5-03, tSorf5-06, tSorf5-14, tSorf6-04, tsorf6-05, tSorf6-07, tSorf6-09, tSorf6-10, tSorf8-03, tSorf8-04, tSorf8-13, tSorf8-14, tSorf8-15, and tSorf8-18 were all selected to evaluate secondary metabolite production.

## Impact of ORF5, ORF6, and ORF8 silencing on PR toxin production and gene expression

PR toxin production by the selected transformants, plasmid control transformant, and parental strain was evaluated in YESC medium after 7-day incubation at 25 °C. Each strain was grown in three biological replicates, and two repetitions were performed. Relative quantification for PR toxin was determined by LC-MS/Q-TOF (Fig. 3) and correlated to the

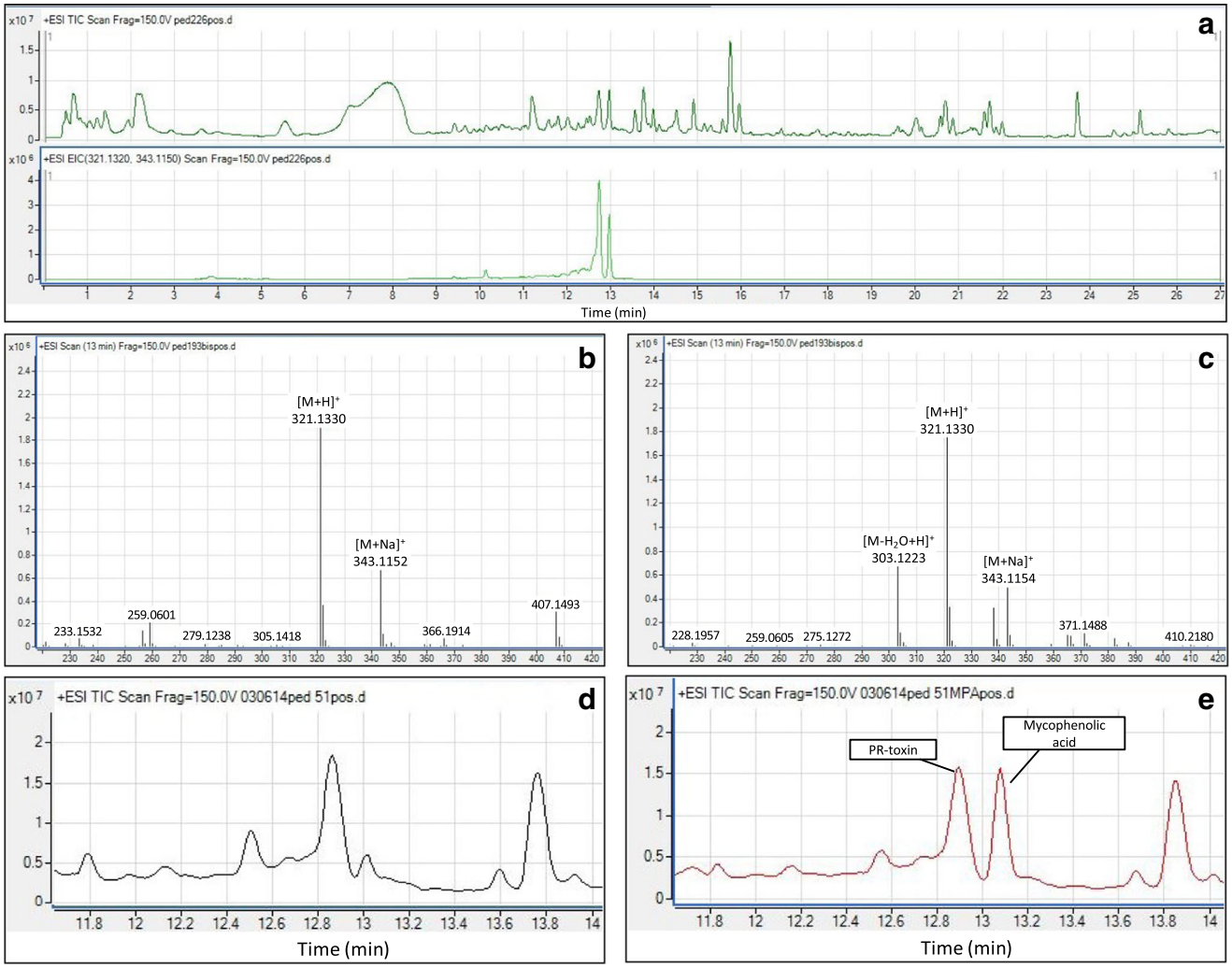


**Fig. 3** **a** HPLC separation of all solvent extracted compounds from a culture of *P. roqueforti* ATCC 48936 (*upper*); extracted ion chromatogram (EIC) of the *m*/*z* value corresponding to PR toxin and mycophenolic acid (321.133 and 343.115) (*lower*). **b** Mass spectrum of the peak with retention time of 12.75 min. **c** Mass spectrum of the peak with retention time of 13.00 min. **d** Total ion current (TIC) chromatogram of crude extract from a culture of *P. roqueforti* ATCC 48936. **e** TIC chromatogram of the sample injected in **d** spiked with mycophenolic acid

mycelium dry masses (no significant differences were observed among the dry mass mean values). The results of PR toxin analysis for each strain and the standard deviations are shown in Fig. 4. No significant differences were observed between the parental strain and control plasmid transformants in the different experiments (all <4%) (data not shown).

Concerning ORF5, four transformants were analyzed and they all showed significant reductions in PR toxin production ranging from 20 to 32%. For the six ORF6 transformants, PR toxin reductions ranged from 23 to 41%, while PR toxin reductions were from 33 to 41% for the six ORF8 transformants. The fact that silencing of the targeted ORF5, ORF6, and ORF8 led to a significant and reproducible decrease in PR toxin production in comparison to the parental strain strongly suggests the involvement of the corresponding genes in PR toxin biosynthesis. To further confirm this finding, RT-qPCR experiments were directly carried out on 4-day-old *P. roqueforti* cultures as RNAi gene silencing is known to have short-term transient effects (one representative transformant was selected per gene target). Gene expression data were analyzed based on the $2^{-\Delta\Delta C}{}_{T}$ method (Livak method) using *pfkA* as reference gene, and fold differences were determined. Melt curve analyses were also carried out to ensure amplification product specificity for all experiments (melt curve temperatures were determined to be 84.5, 84.0, 83.0, and 83.5 ± 0.5 °C for *pfkA*, ORF5, ORF6, and ORF8, respectively). RT-qPCR for each gene target confirmed that the reduced PR toxin biosynthesis observed for the CI01 (ORF5), CII04 (ORF6), and TR03 (ORF8) transformants in comparison to the parental strain was directly correlated to reduced target gene expression (Fig. 5). The highest fold reduction in gene expression was observed for the CII04 transformant targeting a P450 cytochrome monooxygenase that was almost 6-fold lower, while the CI01 and TR03 transformants showed

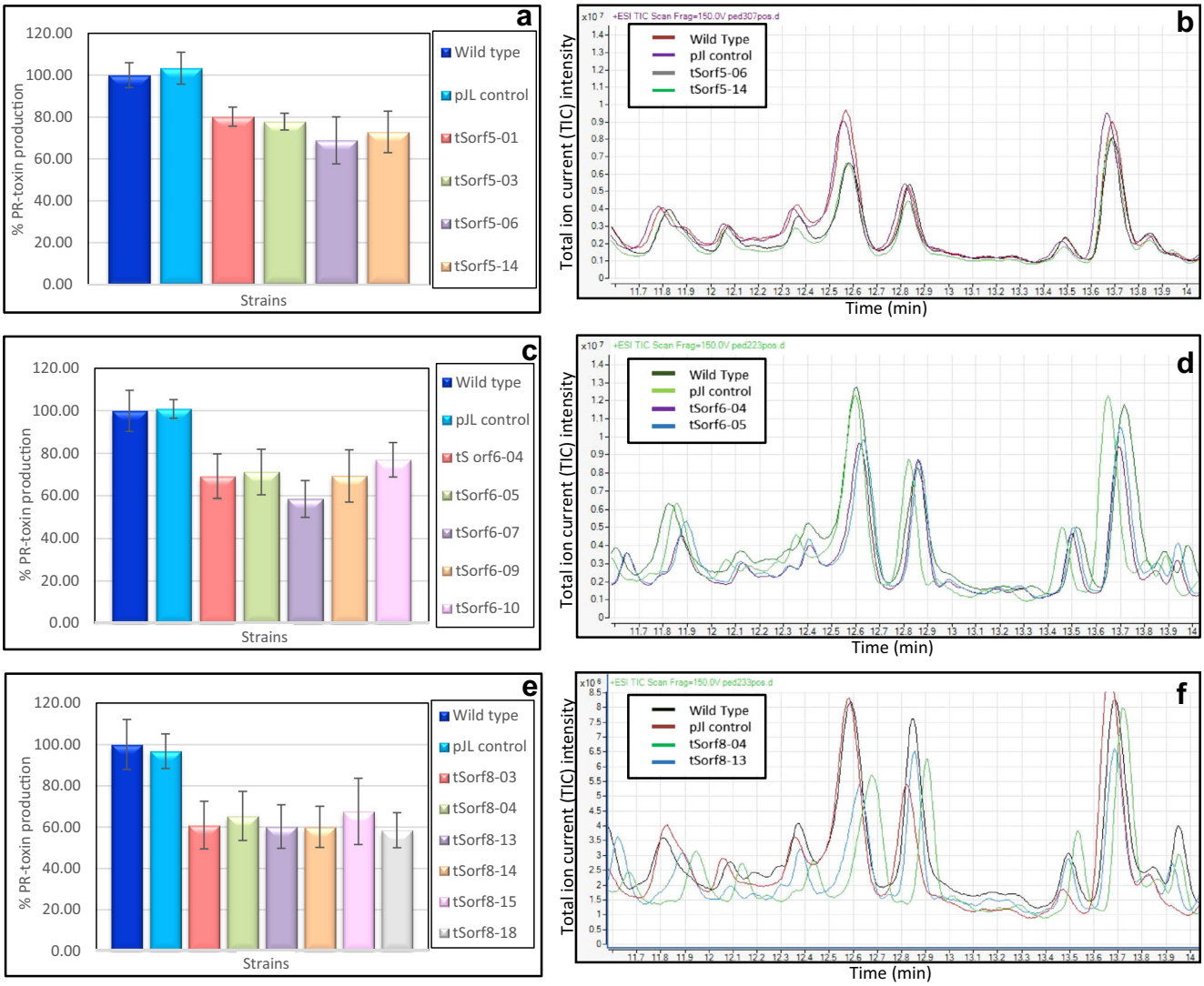


**Fig. 4** Production of PR toxin by the silenced transformants in comparison with the wild-type strain (*P. roqueforti* ATCC 48936) and a transformant with pJL43RNAi plasmid alone (pJL control). **a** ORF5 for wild type; pJL control; and four transformants tSorf5-01, tSorf5-03, tSorf5-06, and tSorf5-14. **c** ORF6 for wild type; pJL control; and five transformants tSorf6-04, tSorf6-05, tSorf6-07, tSorf6-09, and tSorf6-10. **e** ORF8 for wild type; pJL control; and six transformants tSorf8-03, tSorf8-04, tSorf8-13, tSorf8-14, tSorf8-15, and tSorf8-18. **b**, **d**, **f** Total ion current (TIC) chromatograms in ESI+ of all solvent extracted compounds from the *P. roqueforti* ATCC 48936 parental strain (wild type), pJL control, and two representative transformants for ORF5, ORF6 and ORF8, respectively. PR toxin and mycophenolic acid peaks were identified at retention times of approximately 12.60 and 12.85 min, respectively

1.6- and 2.6-fold reductions in P450 cytochrome monooxygenase and transferase gene expression, respectively. Finally, results showed reduced expression for all three gene targets, clearly implying their implication in PR toxin biosynthesis.

Production of two proposed intermediate compounds (eremofortin A (ErmA) and eremofortin B (ErmB)) in PR toxin synthesis by silenced transformants and control strains was also evaluated based on available standards. ErmA production by ORF5, ORF6, and ORF8 transformants is shown in Fig. 6a, c, e and ErmB production in Fig. 6b, d, f. There were no differences in the production of ErmA and ErmB between parental strain and control transformants (tSpJLs) in the different experiments. Noteworthy, ErmA and ErmB productions were both reduced in strains transformed with the pSORF6-RNAi plasmid in the range of 30–40 and 35–43%, respectively. This suggests the involvement of the P450 monooxygenase upstream of ErmB and A formations in the proposed biosynthesis pathway by Hidalgo et al. (2014). Silenced transformants in ORF5 and ORF8 exhibited similar behavior with ErmA reduction (25–30 and 40–45%) but increasing ErmB production (13–33 and 13–23%). This suggested that the corresponding enzymes (a P450 monooxygenase and an acetyltransferase, respectively) intervene after ErmB production and impact ErmA production. One exception was observed for tSorf8-03, as a drastic decrease in production of both intermediary metabolites by 75 and 90%,

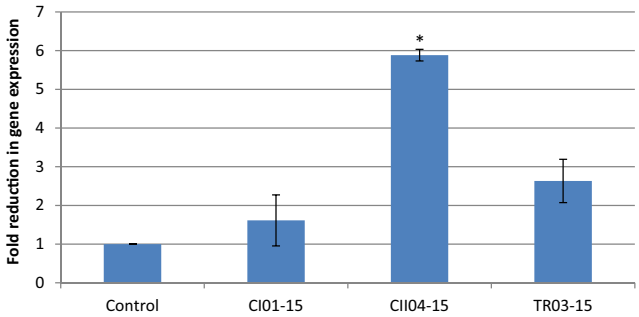


**Fig. 5** Relative gene expression for ORF5 (cytochrome P450 gene), ORF6 (cytochrome P450 gene), and ORF8 (transferase gene) for the CI01, CII04, and TR03 silenced transformants, respectively, compared to the *P. roqueforti* control strain (ATCC 48936) based on the pfkA reference gene. *Error bars* show standard deviations. Significantly different means (*$P < 0.05$) different from the control are represented by an *asterisk*

respectively, was observed and can likely be explained by the RNA interference methodology used. Indeed, this method is known to create in some cases off-target responses, and therefore, it is of utmost importance to systematically analyze multiple transformants for a given gene to ensure reproducible and robust results.

Based on these results and those recently obtained in previous studies (Hidalgo et al. 2014; Riclea and Dickschat 2015), the possible involvement of the so far studied ORFs in the PR toxin biosynthetic pathway is presented in Fig. 7.

## Discussion

Through an in silico analysis of the recently sequenced *P. roqueforti* FM164 genome, this study describes for the first time the gene cluster putatively involved in PR toxin biosynthesis in *P. roqueforti*. The PR toxin biosynthetic cluster spans an approximately 24-kb region in the *P. roqueforti* FM164

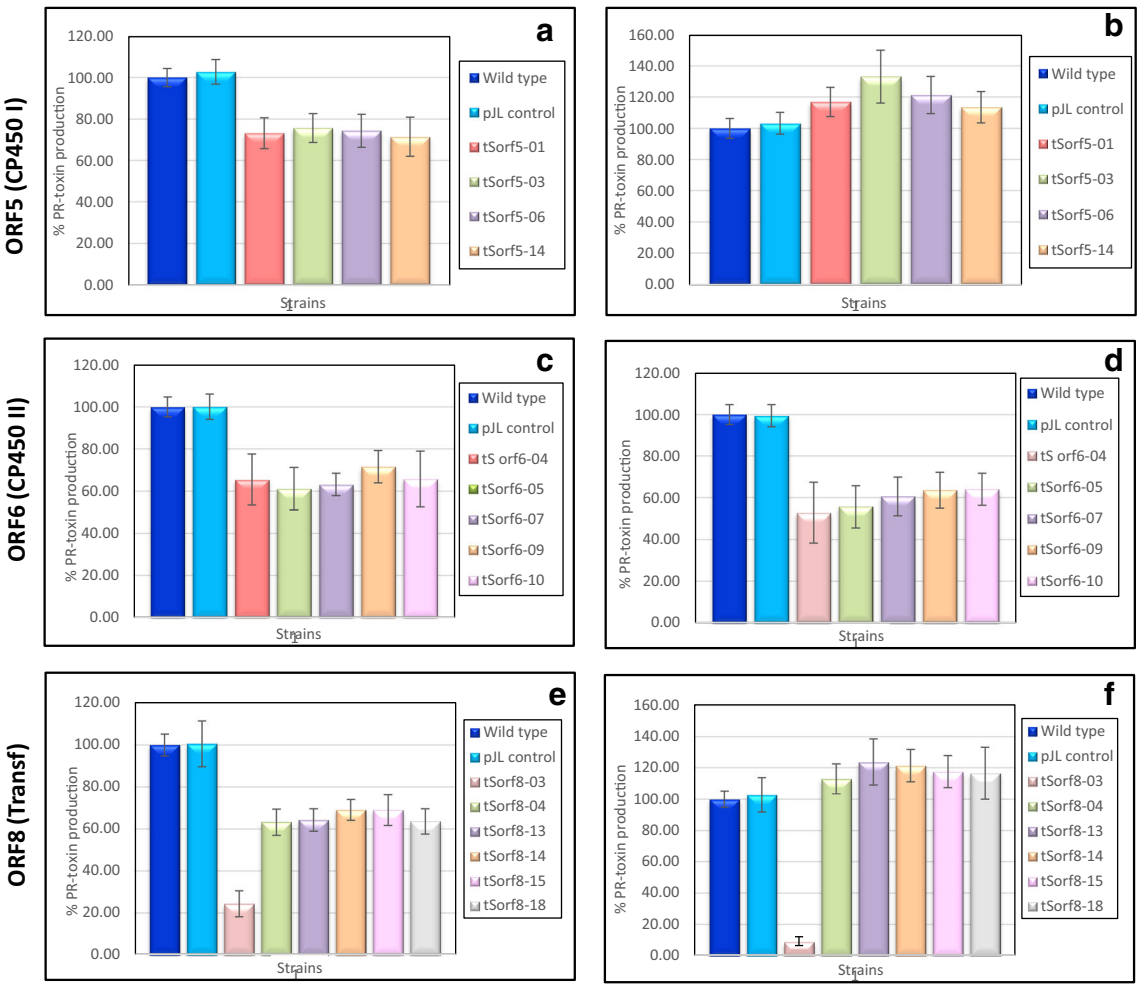


**Fig. 6** Production of eremofortins A and B by the silenced transformants in comparison with the wild-type strain (*P. roqueforti* ATCC 48936) and a transformant with pJL43RNAi plasmid alone (pJL control). **a** ErmA production in tSorf5s, **b** ErmB in tSorf5s, **c** ErmA in tSorf6s, **d** ErmB in tSorf6s, **e** ErmA in tSorf8s, and **f** ErmB in tSorf8

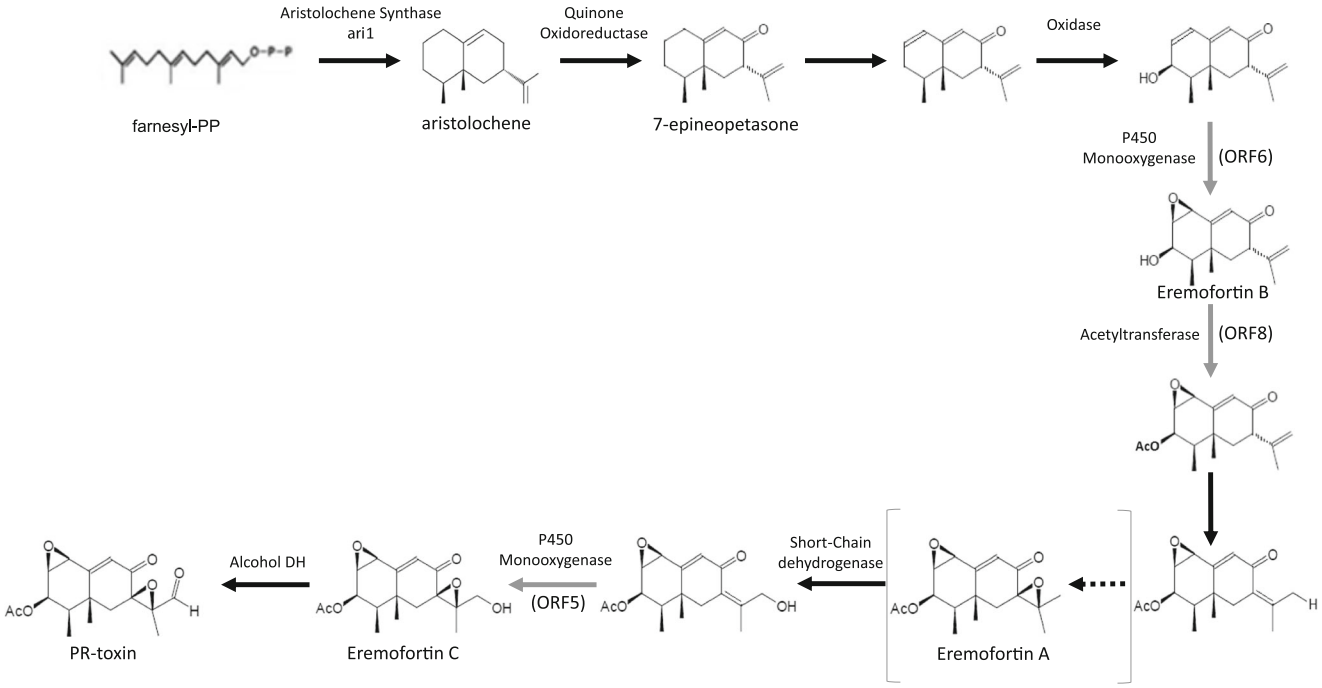


**Fig. 7** Proposed PR toxin biosynthetic pathway in *P. roqueforti*. *Gray arrows* represent the three genes (ORF5, ORF6, and ORF8) targeted for gene silencing experiments in this study

genome and contains 11 putative open reading frames. Beyond the well-known *ari*1 gene encoding the aristolochene synthase, the cluster analysis allowed for the confirmation of the presence of three other genes recently identified by Hidalgo et al. (2014). These genes corresponded to a quinone oxidase (ORF3) and two dehydrogenases (ORF1 and ORF4). Seven other ORFs were identified, and while ORF7 was associated with a protein family of unknown function (DUF3237 superfamily), all others could be assigned to a known function. Significantly, four of the remaining ORFs corresponded to P450 monooxygenases (ORF5, ORF6, ORF9, and ORF11), one to a transferase (ORF8) and one to a transcriptional regulatory gene (ORF10), the latter probably being involved in regulation of the gene cluster transcription and, therefore, PR toxin production. In this context, it would be of particular interest to look into why *P. camemberti* does not produce this mycotoxin as a similar cluster was identified.

To better understand the *P. roqueforti* PR toxin biosynthesis pathway, the previously described RNA interference strategy used to study mycotoxin biosynthesis pathways (including PR toxin) in *P. rubens* (Ullán et al. 2008) and *P. roqueforti* (Hidalgo et al. 2014; Kosalková et al. 2015) was used. The ORF 5 (P450 monooxygenase), ORF6 (P450 monooxygenase), and ORF8 (transferase) were targeted in this study. Relative quantitative analyses from replicate fermentations all showed significant and consistent decreases in PR toxin production for all transformants in comparison to the parental strain, thereby confirming the involvement of all three genes in PR toxin biosynthesis in this species. Noteworthy, among *P. roqueforti* mycotoxins, PR toxin and MPA are peculiar. Indeed, although these two compounds are structurally very different and have a slightly different polarity, they have the same molecular formula ($C_{17}H_{20}O_6$) and molecular mass (320.3371 g $mol^{-1}$) (O'Brien et al. 2006). These features coupled with the fact that no PR toxin standard is currently commercially available make it very difficult to identify and quantify this mycotoxin. However, MPA being commercially available, comparison of the LC-MS/Q-TOF chromatograms obtained in ESI+ for a crude extract from a culture of *P. roqueforti* (Fig. 3) and the same extract spiked with the MPA standard (Fig. 3e) allowed for unequivocal identification of the PR toxin and MPA-associated peaks, thereby allowing us to selectively quantify this metabolite. Moreover, PR toxin is not detected in ESI− ionization conditions, while the MPA $[M-H]^-$ (*m*/*z* 319) ion was detected (data not shown). Finally, in the context of this study, a PR toxin sample prepared by Dr. O. Puel (Toxalim, INRA, France) allowed for final assignation.

Two intermediates, ErmA and ErmB (for which standards are commercially available), were also monitored in fermentation samples. Reduced production of both intermediates was detected in strains transformed with the plasmid pSORF6-RNAi; this silencing cassette targeted the first gene coding for a putative P450 monooxygenase in this pathway (as described by Hidalgo et al. 2014) and that is likely to be directly involved in ErmB production, thus confirming our RNAi results. On the other hand, RNAi silencing cassettes used to target ORF5 (coding for the second P450 monooxygenase in the pathway) and ORF8 (coding for a putative acetyltransferase) showed consistently reduced ErmA levels and, on the contrary, ErmB accumulation among transformants in comparison to the parental strain. These results are again consistent with our RNAi

experimental data and the two pathway gene targets recently described in the proposed biosynthesis pathway by Hidalgo et al. (2014). This also suggests the involvement of both eremofortins as intermediates in PR toxin biosynthesis. The implication of ErmA as a PR toxin pathway intermediate was recently questioned in a study by Riclea and Dickschat (2015) involving feeding experiments with $^{13}$C-labeled precursors. In the latter study, they suggested that ErmA was likely a shunt product; in this case, ErmA would accumulate during PR toxin production. However, in our study, ErmA production was consistently lower in the studied transformants (regardless of the target gene), which rather favors the hypothesis that this compound is indeed a pathway intermediate and likely involved in the last steps of PR toxin production. Further studies will be required to fully elucidate this pathway. Noteworthily, PR toxin reduction levels as well as those obtained for ErmA and B slightly varied among transformants. This finding has already been shown in other RNAi knockdown studies (Janus et al. 2007; Ullán et al. 2008; Hidalgo et al. 2014). Moreover, RNAi results are considered to be transient (Salame et al. 2010) and this approach is not site directed, which can lead in some cases to contrasted off-target effects. These facts highlight the interest for easy-to-use knockout strategies for fungi for the future.

As previously stated, a biosynthesis pathway for PR toxin production was recently proposed by Hidalgo et al. (2014). The latter study described putative pathway intermediates including the eremofortins A, B, and C as well as the potential functions of the potential genes and enzymes likely to be involved in PR toxin biosynthesis although not all interconversions are fully clear. To further understand PR toxin biosynthesis in this species, Riclea and Dickschat (2015), via (11, 12, 13-$^{13}C_3$)-7-*epi*-neopetasone feeding experiments, proposed an updated biosynthesis pathway as a potential working hypothesis. In particular, their results revealed that 7-*epi*-neopetasone is a new pathway intermediate and this compound would be converted from aristolochene via an allylic oxidation. Moreover, its instability may play a role in the corresponding spontaneous double-bond migration during PR toxin biosynthesis (Riclea and Dickschat 2015). Again, these authors also stipulate that eremofortins B and C would be pathway intermediates, while eremofortin A may rather be a shunt product that likely arises from premature epoxidation of one of the other pathway intermediates. Our data are also in agreement with eremofortin B as a pathway intermediate, but questions can still arise as to whether eremofortin A is a shunt product or an intermediate as suggested by our results. Further studies are clearly required to fully elucidate all the steps involved in PR toxin biosynthesis and determine if the other determined ORFs are indeed implicated and at which step.

In conclusion, the results obtained on the PR toxin biosynthesis pathway allowed gaining knowledge on the role of the different genes in the identified 11 gene clusters. These data combined with biochemical production data could also be used for future strain selection. Indeed, recent findings in our laboratory have shown highly strain-dependent PR toxin production abilities among 55 *P. roqueforti* strains of different genetic and/or environmental origins.

**Acknowledgements** The authors would like to thank Dr. Olivier Puel from INRA Toulouse for useful discussion on PR toxin identification and for kindly providing a PR toxin sample. We are also grateful to Pr. Joëlle Dupont from the MNHN for providing the *P. roqueforti* FM164 genome sequence, Nolwenn Hymery for RT-qPCR statistical analyses, and Riccardo Baroncelli for bioinformatics assistance for PR toxin clusters.

**Compliance with ethical standards**

**Funding** This study was supported by funding from the Région Bretagne, France (PENIMET 7923, Stratégie d'Attractivité Durable), to Monika Coton for a post-doctoral fellowship for Pedro Hidalgo.

**Conflict of interest** All authors declare that they have no conflict of interest.

**Ethical approval** This article does not contain any studies with human participants or animals performed by any of the authors.

## References

Abe K, Gomi K, Hasegawa F, Machida M (2006) Impact of *Aspergillus oryzae* genomics on industrial production of metabolites. Mycopathologia 162:143–153. doi:10.1007/s11046-006-0049-2

Altschul SF, Gish W, Miller W, Myers EW, Lipman DJ (1990) Basic local alignment search tool. J Mol Biol 215:403–410

Boysen ME, Jacobsson KG, Schnürer J (2000) Molecular identification of species from the *Penicillium roqueforti* group associated with spoiled animal feed. Appl Environ Microbiol 66:1523–1526

Brock NL, Dickschat JS (2013) PR toxin biosynthesis in *Penicillium roqueforti*. Chem Bio Chem 14:1189–1193

Cantor M, van der Tempel M, Hasen T, Ardö Y (2004) Blue cheese in: Cheese: chemistry physics and microbiology. Elsevier, Oxford, pp. 175–199

Caruthers JM, Kang I, Rynkiewicz MJ, Cane DE, Christianson DW (2000) Crystal structure determination of aristolochene synthase from the blue cheese mold *Penicillium roqueforti*. J Biol Chem 275:25533–25539

Casqueiro J, Gutiérrez S, Bañuelos O, Hijarrubia MJ, Martín JF (1999) Gene targeting in *Penicillium chrysogenum*: disruption of the lys2 gene leads to penicillin overproduction. J Bacteriol 181:1181–1188

Castellari C, Quadrelli AM, Laich F (2010) Surface mycobiota on Argentinean dry fermented sausages. Int J Food Microbiol 142: 149–155. doi:10.1016/jijfoodmicro201006016

Chang L, Tsai W (1998) Isolation purification and characterization of the PR oxidase from *Penicillium roqueforti*. Appl Environ Microbiol 64:5012–5015

Chang SC, Wei YH, Wei DL, Chen YY, Jong SC (1991) Factors affecting the production of eremofortin C and PR toxin in *Penicillium roqueforti*. Appl Environ Microbiol 57:2581–2585

Chang SC, Lu KL, Yeh SF (1993) Secondary metabolites resulting from degradation of PR toxin by *Penicillium roqueforti*. Appl Environ Microbiol 59:981–986

Chang SC, Yeh SF, Li SY, Lei WY, Chen MY (1996) A novel secondary metabolite relative to the degradation of PR toxin by *Penicillium roqueforti*. Curr Microbiol 32:141–146

Cheeseman K, Ropars J, Renault P, Dupont J, Gouzy J, Branca A, Abraham A-L, Ceppi M, Conseiller E, Debuchy R, Malagnac F, Goarin A, Silar P, Lacoste S, Sallet E, Bensimon A, Giraud T, Brygoo Y (2014) Multiple recent horizontal transfers of a large genomic region in cheese making fungi. Nat. Commun. 5. doi:10.1038/ncomms3876

Chen FC, Chen CF, Wei RD (1982) Acute toxicity of PR toxin a mycotoxin from *Penicillium roqueforti*. Toxicon Off J Int Soc Toxinology 20:433–441

Del-Cid A, Gil-Durán C, Vaca I, Rojas-Aedo JF, García-Rico RO, Levicán G, Chávez R (2016) Identification and functional analysis of the mycophenolic acid Gene cluster of *Penicillium roqueforti*. PLoS One 1(1):e0147047

Dumay R, Jalain F (1982) Le roquefort. Perspectives aveyronnaises éditions, Paris

Fink-Gremmels J (2008) Mycotoxins in cattle feeds and carry-over to dairy milk: a review. Food Addit Contam Part A 25:172–180

Frisvad F, Smedsgaard J, Larsen T, Samson R (2004) Mycotoxins drugs and other extrolites produced by species in *Penicillium* subgenus *Penicillium*. Stud Mycol 49:201–242

Gillot G, Jany J-L, Dominguez-Santos R, Poirier E, Debaets S, Hidalgo P, Ullán R, Coton E, Coton M (2016) Genetic basis for mycophenolic acid production and strain-dependent production variability in *Penicillium roqueforti*. doi:10.1016/j.fm.2016.10.013

Gripon JC (1999) Mould-ripened cheeses in: Fox PF (Ed) Cheese: chemistry. US, Physics and Microbiology. Springer, pp. 111–136

Hidalgo PI, Ullán RV, Albillos SM, Montero O, Fernández-Bodega MÁ, García-Estrada C, Fernández-Aguado M, Martín J-F (2014) Molecular characterization of the PR toxin gene cluster in *Penicillium roqueforti* and *Penicillium chrysogenum*: cross talk of secondary metabolite pathways. Fungal Genet Biol FG B 62:11–24

Hymery N, Vasseur V, Coton M, Mounier J, Jany J-L, Barbier G, Coton E (2014) Filamentous fungi and mycotoxins in cheese: a review. Compr Rev Food Sci Food Saf 13:437–456

Janus D, Hoff B, Hofmann E, Kück U (2007) An efficient fungal RNA-silencing system using the dsRed reporter gene. Appl Environ Microbiol 73:962–970

Kosalková K, Domínguez-Santos R, Coton M, Coton E, García-Estrada C, Liras P, Martín JF (2015) A natural short pathway synthesizes roquefortine C but not meleagrin in three different *Penicillium roqueforti* strains. Appl Microbiol Biotechnol 99:7601–7612. doi:10.1007/s00253-015-6676-0

Lavermicocca P, Valerio F, Visconti A (2003) Antifungal activity of phenyllactic acid against molds isolated from bakery products. Appl Environ Microbiol 69 1 634–1640

Livak KJ, Schmittgen TD (2001) Analysis of relative gene expression data using real-time quantitative PCR and the 2−ΔΔCT method. Methods 25:402–408. doi:10.1006/meth.2001.1262

Le Bars J, Le Bars P (1989) Espèces fongiques des ensilages de mais Risques mycotoxiques. Recl Médecine Vét 165:433–439

Lund F, Filtenborg O, Westall S, Frisvad JC (1996) Associated mycoflora of rye bread. Lett Appl Microbiol 23:213–217

Martín JF, Coton M (2017) Blue cheese: microbiota and fungal metabolites. In: Frias J, Martínez-Villaluenga C, Peñas E (eds) Fermented foods in health and disease prevention. Academic Press, pp 275–303

Modler HW, Brunner JR, Stine CM (1974) Extracellular protease of *Penicillium roqueforti* I production and characteristics of crude enzyme preparation. J Dairy Sci 57:523–527. doi:10.3168/jdsS0022-0302(74)84927-1

Moreau S, Lablache-Combier A, Biguet J (1980) Production of eremofortins a B and C relative to formation of PR toxin by *Penicillium roqueforti*. Appl Environ Microbiol 39:770–776

Nielsen KF, Sumarah MW, Frisvad JC, Miller JD (2006) Production of metabolites from the *Penicillium roqueforti* complex. J Agric Food Chem 54:3756–3763

O'Brien M, Nielsen KF, O'Kiely P, Forristal PD, Fuller HT, Frisvad JC (2006) Mycotoxins and other secondary metabolites produced *in vitro* by *Penicillium paneum* Frisvad and *Penicillium roqueforti* Thom isolated from baled grass silage in Ireland. J Agric Food Chem 54:9268–9276. doi:10.1021/jf0621018

Okado N, Sugi M, Ueda M, Mizuhashi F, Lynch BS, Vo TD, Roberts AS (2015) Safety evaluation of AMP deaminase from *Aspergillus oryzae*. Food Chem Toxicol Int J Publ Br Ind Biol Res Assoc. doi:10.1016/jfct201511001

Polonelli L, Morace G, delle Monache F, Samson RA (1978) Studies on the PR toxin of *Penicillium roqueforti*. Mycopathologia 66:99–104

Proctor RH, Hohn TM (1993) Aristolochene synthase. Isolation, characterization and bacterial expression of a sesquiterpenoid biosynthetic gene (Ari1) from *Penicillium roqueforti*. J Biol Chem 268:4543–4548

Rasmussen RR, Storm IMLD, Rasmussen PH, Smedsgaard J, Nielsen KF (2010) Multi-mycotoxin analysis of maize silage by LC-MS/MS. Anal Bioanal Chem 397:765–776

Riclea R, Dickschat JS (2015) Identification of intermediates in the biosynthesis of PR toxin by *Penicillium roqueforti*. Angew Chem Int Ed 54:1–5

Salame TM, Ziv C, Hadar Y, Yarden O (2010) RNAi as a potential tool for biotechnological applications in fungi. Appl Microbiol Biotechnol 89:501–512

Scott R (1986) Cheesemaking practice. Elsevier Applied Science Publishers

Scott PM, Kanhere SR (1979) Instability of PR toxin in blue cheese. J-Assoc Off Anal Chem 62:141–147

Scudamore KA, Livesey CT (1998) Occurrence and significance of mycotoxins in forage crops and silage: a review. J Sci Food Agric 77:1–17

Shetty AS, Gaertner FH (1975) Kynureninase-type enzymes of *Penicillum roqueforti, Aspergillus niger*, *Rhizopus stolonifer* and *Pseudomonas fluorescens*: further evidence for distinct kynureninase and hydroxykynureninase activities. J Bacteriol 122:235–244

Starzynska-Janiszewska A, Stodolak B, Dulinski R, Mickowska B (2012) The influence of inoculum composition on selected bioactive and nutritional parameters of grass pea tempeh obtained by mixed-culture fermentation with *Rhizopus oligosporus* and *Aspergillus oryzae* strains. Food Sci Technol Int Cienc Tecnol Los Aliment Int 18:113–122

Still P, Wei R, Smalley E, Strong F (1972) A mycotoxin from *Penicillium roqueforti* isolated from toxic cattle feed. Fed Proc 31:733

Storm IMLD, Kristensen NB, Raun BML, Smedsgaard J, Thrane U (2010) Dynamics in the microbiology of maize silage during whole-season storage. J Appl Microbiol 109:1017–1026

Storm IMLD, Rasmussen RR, Rasmussen PH (2014) Occurrence of pre- and post-harvest mycotoxins and other secondary metabolites in Danish maize silage. Toxins 6:2256–2269

Ullán RV, Campoy S, Casqueiro J, Fernández FJ, Martín JF (2007) Deacetylcephalosporin C production in *Penicillium chrysogenum* by expression of the isopenicillin N epimerization ring expansion and acetylation genes. Chem Biol 14:329–339

Ullán RV, Godio RP, Teijeira F, Vaca I, García-Estrada C, Feltrer R, Kosalkova K, Martín JF (2008) RNA-silencing in *Penicillium chrysogenum* and *Acremonium chrysogenum*: validation studies using beta-lactam genes expression. J Microbiol Methods 75:209–218

Veselý D, Veselá D, Adámková (1981) Occurrence of PR toxin-producing *Penicillium roqueforti* in corn silage. Vet Med 26:109–115

Wei R, Schnoes H, Hart P, Strong F (1975) The structure of PR toxin a mycotoxin from *Penicillium roqueforti*. Tetrahedro 31:109–114

Wei R, Ong T, Whong W, Frezza D, Bronzetti G, Zeiger E (1979) Genetic effects of PR toxin in eukaryotic microorganisms. Environ Mutagen 1:45–53